scientific reports

Check for updates

OPEN

MYH6 suppresses tumor progression by downregulating KIT expression in human prostate cancer

Fei Wang[1,2], Hua Shen[1,2], Kai Li[1], Yanhong Ding[1], Jianqing Wang[1]✉ & Jian Sun[1]✉

Prostate cancer (PRAD) is one of the leading malignancies in men all around the world. Here, we identified Myosin Heavy Chain 6 (MYH6) as a potential tumor suppressor gene in the development of prostate cancer. We found lower expression of MYH6 in prostate cancer tissues, and its lower gene expression was also associated with worse clinical outcomes. In vitro and in vivo assays indicated that overexpressed MYH6 could suppress the proliferation and migration progression of prostate cancer cells. RNA-seq was employed to investigate the mechanism, and KIT Proto-Oncogen (KIT) was determined as the downstream gene of MYH6, which was further confirmed using rescue assays. In all, we provide the evidence that MYH6 could serve as a tumor suppressor in prostate cancer. Our results highlight the potential role of MYH6 in the development of prostate cancer.

Keywords MYH6, Prostate cancer, Prognostic marker, Tumor suppressor gene

Prostate cancer, the most prevalent malignancy among men globally, continues to pose significant challenges to both researchers and clinicians[1]. Despite advancements in our understanding of the disease and its therapeutic strategies, the underlying molecular mechanisms contributing to prostate cancer progression remain incompletely elucidated.

MYH6 (myosin heavy chain 6) gene encodes alpha heavy chain subunit of cardiac myosin (αMyHC)[2]. It is primarily known for its critical role in cardiac muscle contraction and has garnered attention for its potential involvement in various cellular processes beyond the heart[3]. While the majority of studies have focused on MYH6's cardiac function, its relevance in noncardiac tissues, including the prostate, is an intriguing avenue of research[4]. In cancer research, previous studies have found that MYH6 is significantly downregulated in head and neck squamous cell carcinoma[5]. In small cell lung cancer (SCLC), MYH6 is frequently mutated in chemotherapy-treated residual tumors, which might contribute to chemoresistance and influence the prognosis of patients[6]. Our previous studies also found that in PTEN-mutated or TP53-mutated prostate cancer, MYH6 acts as a hub gene and plays a potential role[7,8].

Here we attempted to identify novel critical genes that might lead to prostate cancer development. We overlapped the hub genes in our previous studies and online datasets and found that MYH6 was the hub gene in both the groups. Subsequently, our attention turned towards MYH6, with the aim of thoroughly investigating its involvement in the development of prostate cancer, unveiling its potential as an innovative biomarker and target for therapeutic interventions. Understanding the mechanistic underpinnings of MYH6 involvement in prostate cancer might open new avenues for personalized treatment strategies and improve the overall management of this formidable malignancy.

Materials and methods

Identification of MYH6 and online data information

To identify important genes involved in prostate cancer development, we reviewed the hub genes from our previous studies[7,8], and analyzed the DEGs in the GDS1439 prostate cancer database. Through integrated bioinformatics analysis, we found that MYH6 was the only intersecting gene among the three datasets, confirming it as our target gene. Subsequently, we used GEPIA2 to examine the expression pattern of MYH6 across various cancer types and analyzed data on overall survival (OS) and disease-free survival (DFS), as well as survival plots

[1]Department of Urology, The Affiliated Suzhou Hospital of Nanjing Medical University, Suzhou Municipal Hospital, Gusu School, Nanjing Medical University, 26 Daoqian Rd, Suzhou 215000, Jiangsu, People's Republic of China. [2]These authors contributed equally: Fei Wang and Hua Shen. ✉email: jqwang14@fudan.edu.cn; drsunjian1978@163.com

related to MYH6 in different types of tumors. Gene expression profiles of prostate cancer and normal tissues were downloaded from GSE35988 and GDS1439, respectively, in the NCBI-GEO database. GSE35988 and GDS1439 are two classic public databases for prostate cancer, containing a wealth of sequencing data and clinical data from patients with prostate cancer. GSE35988 includes matched benign prostate tissues (n = 28), localized prostate cancer (n = 59), and metastatic castrate-resistant prostate cancer (CRPC, n = 35). GDS1439 includes 19 cases of benign, clinically localized prostate cancer tumors, as well as metastatic and hormone-refractory prostate cancer tumors. In the analysis, EdgeR was used for examining DEGs as previously described[9,10]. DEGs were identified based on the following criteria: fold change (FC) ≥ 2 or ≤ 0.5; P value and false discovery rate (FDR) < 0.05.

Patient information

Tissue samples from 75 prostate cancer patients, along with adjacent paracancerous tissues, were collected for this study. Following surgical removal, all tissues were fixed in formalin. The study obtained approval from the Ethics Committee of Nanjing Medical University, and all participants provided written informed consent prior to their participation.

Immunohistochemistry (IHC)

We obtained and handled adjacent and prostate cancer tissues following previously established protocols[11]. Immunohistochemistry (IHC) was carried out as detailed elsewhere[12,13]. In short, slides underwent deparaffinization followed by antigen retrieval via heating in citrate buffer with a pH of 6. The primary antibodies were MYH6 (YT6101, Immunoway) and KIT (ab260048, Abcam), respectively. Immunohistochemical staining was performed using the streptavidin-biotin-peroxidase technique, with diaminobenzidine employed as the chromogen. We omitted the primary antibody or incubated with a not related antibody to obtained negative controls.

MYH6 staining was evaluated independently by two observers, one of whom was a pathologist. Finally, we would have a consensus score for each tissue. MYH6-positive reactions were graded into four levels based on staining intensity (0, 1, 2, and 3). The percentage of MYH6-positive cells was divided into four categories: 0 (0%), 1 (1–33%), 2 (34–66%), and 3 (67–100%). In cases of discrepancies in core scores, the higher score between the two tissues was adopted as the final score. The final staining score was obtained by adding up the intensity and percentage scores. Staining patterns were classified as follows: 0 for negative, 1 to 2 for weak, 3 to 4 for moderate, and 5 to 6 for strong[14].

Cell culture

We sourced LNCaP, PC-3 and DU145 cells, two classic prostate cancer cells, from ATCC (Bethesda, USA). The cells underwent culturing in RPMI-1640 medium supplemented with 10% FBS and antibiotics (0.1 mg/ml streptomycin and 100 units/ml penicillin), following the protocol outlined in prior literature[15]. The authentication process for all cell lines employed in our study involved STR profiling, and thorough testing was performed to ensure absence of mycoplasma contamination.

Construction of stable cell lines

We addressed the constructs as previously described[15,16]. We ligated full-length MYH6 into pPB-CAG-ires-Pac vector to construct pPB-CAG-MYH6-ires-Pac. The stable cell lines for MYH6 overexpression, serving as the control, were acquired using the same methodology as previously described[15]. Western blot analysis was performed to identify and verify the presence of stable cell lines.

Antibodies and immunoblotting

For western blotting, the cells were lysed in 1× SDS loading buffer (50 mM Tris–HCl pH 6.8, 10% glycerol, 2% SDS, 0.05% bromophenol blue and 1% 2-mercaptoethanol). The following antibodies were used: anti-MYH6 (YT6101, Immunoway), anti-KIT (HY-P80619, MCE), anti-FLAG (20543-1-AP, Proteintech), and anti-ACTIN (20536-1-AP, Proteintech). Immunoblotting was performed as previously described[15]. Briefly, all proteins were separated by SDS-PAGE and transferred to polyvinylidene difluoride membranes (Millipore). HRP-labeled secondary antibodies and enhanced chemiluminescence system was used for signal detection. The protein was visualized an using imaging system (Odyssey).

Cell proliferation (MTS) assay

The cell proliferation assay was conducted following previously established protocols[17]. In summary, cells were plated at a density of 4000 cells per well in 96-well plates and cultured at 37 °C for 6 days. At specified intervals, cells received treatment with 20 µl of CellTiter 96 AQueous One solution reagent (Promega) diluted in 100 µl of medium for 1 h. Cell quantification was then conducted using a microplate reader (Biotek).

RNA-seq and analysis

In our study, we obtained total RNAs from cells using TRIzol reagent (Invitrogen) and eliminated any genomic DNA using DNase I (TaKara). Subsequently, RNA was quantified using ND-2000 (NanoDrop Technologies). For further analysis, only RNA samples of exceptional quality meeting the specific criteria (OD260/280 = 1.8–2.2, OD260/230 ≥ 2.0, RIN ≥ 6.5, 28S:18S ≥ 1.0, > 10 µg) were chosen to construct the sequencing library. The RNA-seq libraries were then processed on the Illumina HiSeq 4000 sequencing platform at Shanghai Majorbio Bio-pharm Technology Co., Ltd (China).

Identification of differentially expressed genes (DEGs)

EdgeR was used for examining DEGs as previously described[9,10]. DEGs were identified based on the following criteria: fold change (FC) ≥ 2 or ≤ 0.5; P value and false discovery rate (FDR) < 0.05. These DEGs were subjected to additional bioinformatics analysis.

Cell migration assays

We employed a Transwell system (Corning) in 24-well tissue culture plates to conduct cell migration assays, following previously established protocols[15].

Real-time RT-PCR assays

In the present study, total RNA was isolated from cultured cells employing TRIzol reagent (Invitrogen). This extracted RNA was then reverse transcribed using reverse transcriptase (Fermentas). Quantitative real-time PCR was conducted utilizing the Bio-Rad CFX96 system, with relative gene expression normalized against GAPDH as a control. The primer sequences employed in this study are listed below:

MYH6-F: GCCCTTTGACATTCGCACTG;
MYH6-R: GGTTTCAGCAATGACCTTGCC;
GAPDH-F: GGAGCGAGATCCCTCCAAAAT
GAPDH-R: GGCTGTTGTCATACTTCTCATGG.

In vivo tumor growth assay

For the tumor growth assay, we subcutaneously inoculated 1×10^6 cells into six-week-old male athymic mice. Each group, comprising the control group and the MYH6-OE group, consisted of seven mice, and all mice were sacrificed after 4 weeks. All the tumors were monitored twice a week, with tumor sizes measured and recorded as length × width^2 × 0.5 (mm^3). All animal use procedures were approved by the Ethics Committee of Nanjing Medical University.

Functional annotation and pathway enrichment analysis

We utilized the Database for Annotation, Visualization, and Integrated Discovery (DAVID) website to conduct Gene Ontology (GO) analysis and Kyoto Encyclopedia of Genes and Genomes (KEGG) analysis[18–21], with a specified statistical significance threshold of P value < 0.05.

Statistical analysis

All results are presented as mean ± standard error of the means (SEMs). Group differences were evaluated using Student's *t*-test. To analyze the relationship between MYH6 expression and prognosis, we utilized the Kaplan–Meier method and log-rank test in GraphPad. Additionally, we performed Receiver Operating Characteristic (ROC) curve analysis using GraphPad. The Areas Under the Curves (AUCs) were employed to evaluate the diagnostic utility of each marker combination. AUC values exceeding 0.9 were indicative of excellent diagnostic efficacy, while those falling between 0.7 and 0.9 suggested good diagnostic efficacy. Furthermore, False Discovery Rate (FDR) in edgeR and Gene Set Enrichment Analysis (GSEA) were adjusted for multiple testing via the Benjamini–Hochberg procedure to control FDR[22,23]. Statistical significance was defined as having a significance level of P < 0.05. All statistical analyses were conducted using GraphPad and R 3.3.0.

Ethics approval

The authors assert that they have secured proper approval from the Ethics Committee of Nanjing Medical University and have followed the principles outlined in the Declaration of Helsinki for all human or animal experimental investigations. Our study was reported as described by the ARRIVE guidelines (Ethics approval reference number: 20210329).

Results

Identification of MYH6 as the critical gene in prostate cancer

To identify some critical genes in prostate cancer development, we used the data from our previous studies[7,8]. In these studies, we identified some hub genes among the DEGs. Subsequently, we conducted an analysis of the prostate cancer gene expression profiles within GDS1439, identifying DEGs through in silico methods, employing a significance threshold of P < 0.05 and a fold change (FC) criterion of ≥ 2.0 or ≤ 0.5. Following integrated bioinformatics scrutiny, only one gene, MYH6, emerged as significant among the hub genes and DEGs within the dataset (Fig. 1A).

MYH6 plays a tumor suppressor role in most cancer types

MYH6 is a cardiac-related gene whose role in cancer is not quite clear. Then, we first analyzed the role of MYH6 across cancers. We first explored the difference in MYH6 expression between tumor and normal tissues in different cancer types via TIMER2 online tools. As shown in Fig. 1B, MYH6 was downregulated in PRAD, head and neck squamous cell carcinoma (HNSC) and kidney chromophobe (KICH).

Genetic alterations usually contribute to cancer development. We then tried to analyze the influence of MYH6 genetic alterations in human cancers. The frequency of MYH6 alteration in lung cancer was the highest. Other cancers, including non-small cell lung cancer, melanoma, pancreatic cancer, and head and neck cancer, have a higher frequency of MYH6 alteration (> 5%, Fig. 1C). In Fig. 1C, we show the indicated mutations and

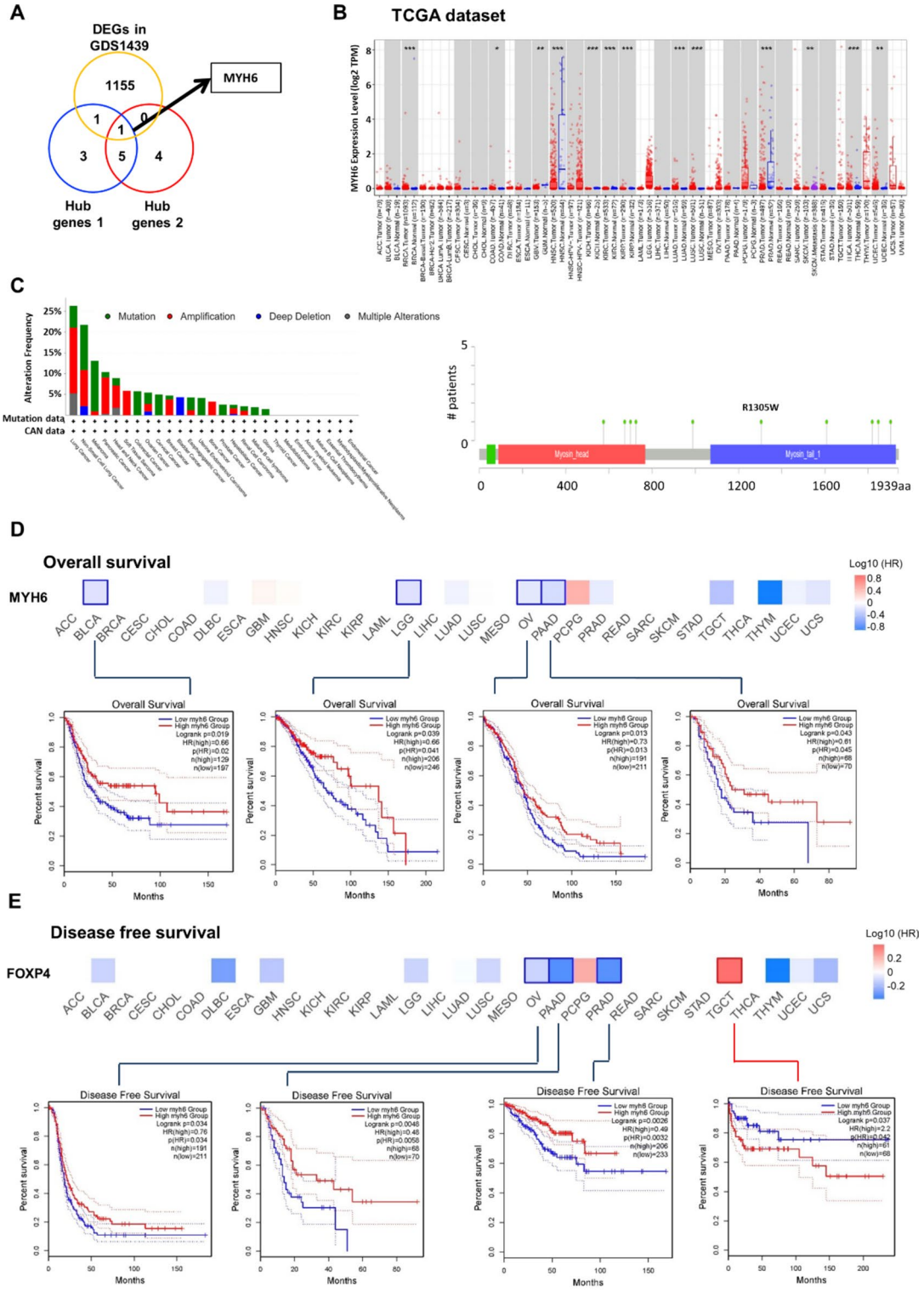

Fig. 1. Identification of MYH6 and its expression level and its correlation with prognosis in different tumors. (**A**) Identification of MYH6 from the hub genes of our two previous studies and one online cohort profile dataset (GDS1439). (**B**) The expression status of the MYH6 gene in different cancers or specific cancer subtypes. *P < 0.05; **P < 0.01; ***P < 0.001. (**C**) Mutation frequency, mutation type and mutation site of MYH6 in TCGA tumors. (**D**) Relationship between MYH6 gene expression and overall survival. (**E**) Relationship between MYH6 gene expression and disease-free survival.

the location in MYH6. Then, we wondered whether MYH6 expression correlated with prognosis. We divided the cases into MYH6 high and low-expression groups according to MYH6 mRNA level. Then, we investigated whether MYH6 expression influenced the disease outcome of patients using data from TCGA datasets. We found that high MYH6 expression levels indicated better prognosis in most cancer types. The OS results showed that high MYH6 correlated with better outcomes for bladder cancer (BLCA), brain lower grade glioma (LGG), ovarian serous cystadenocarcinoma (OV) and pancreatic adenocarcinoma (PAAD) (Fig. 1D). For DFS analysis, we found that higher MYH6 expression correlated with worse outcomes for testicular germ cell tumor (TGCT) but better outcomes in OV, PAAD and PRAD (Fig. 1E).

MYH6 expression was negatively correlated with prostate cancer progression

We then focused on the roles of MYH6 in prostate cancer. We first show the expression patterns of MYH6 in different prostate cancer datasets in Fig. 2A. To assess the diagnostic potential of MYH6 in prostate cancer, we conducted ROC curve analysis for MYH6 using data from GSE35988, comparing healthy individuals with PCa patients. The findings depicted in Fig. 2B indicate that MYH6 holds diagnostic utility for prostate cancer patients. Furthermore, apart from RNA-level analysis, we investigated MYH6 expression at the protein level through immunohistochemistry (IHC) in both prostate cancer and matched paracancerous tissues. As we showed in Fig. 2C, prostate cancer tissues showed much lower MYH6 expression than benign prostatic epithelia. Furthermore, we discovered that prostate cancer patients exhibiting lower levels of MYH6 in their tumor tissues experienced poorer outcomes (Fig. 2D). These findings collectively indicate a positive correlation between reduced MYH6 expression, advanced stage, heightened metastasis, and unfavorable prognosis among prostate cancer patients.

MYH6 could suppress prostate cancer proliferation and migration

To deeply investigate the biological implications of MYH6 in prostate cancer advancement, we enhanced the expression of MYH6 in LNCaP, DU145 and PC-3 prostate cancer cell lines (Fig. 3A and Sup Fig. 1A). Next, we evaluated the effect of MYH6 on the proliferation of prostate cancer cells. In vitro assays revealed that the elevation of MYH6 expression suppressed cell proliferation (Fig. 3B). Transwell assays also showed that overexpression of MYH6 decreased cell migration ability (Fig. 3C). To assess the effects in vivo, we generated a xenograft tumor model using DU145 cells. The results confirmed that overexpression of MYH6 could damage the growth of tumors in vivo (Fig. 3D). These results suggest the tumor suppressor role of MYH6 in prostate cancer.

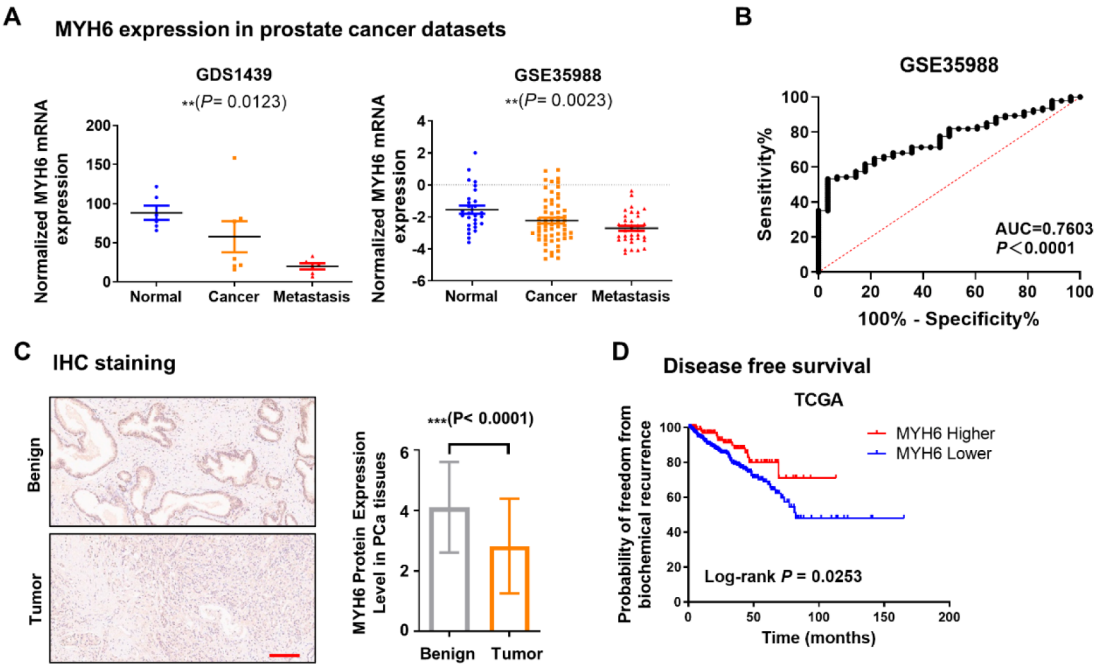

Fig. 2. MYH6 expression is associated with prostate cancer progression severity and prognosis. (**A**) MYH6 mRNA expression levels in prostate cancer samples from GDS1439 and GSE35988. One-way ANOVA was used. (**B**) ROC curves of MYH6 expression in prostate cancer patients. (**C**) Representative immunohistochemistry of MYH6 on benign prostate and prostate cancer tissues. (**D**) Kaplan–Meier survival curves for prostate cancer patients stratified by MYH6 expression.

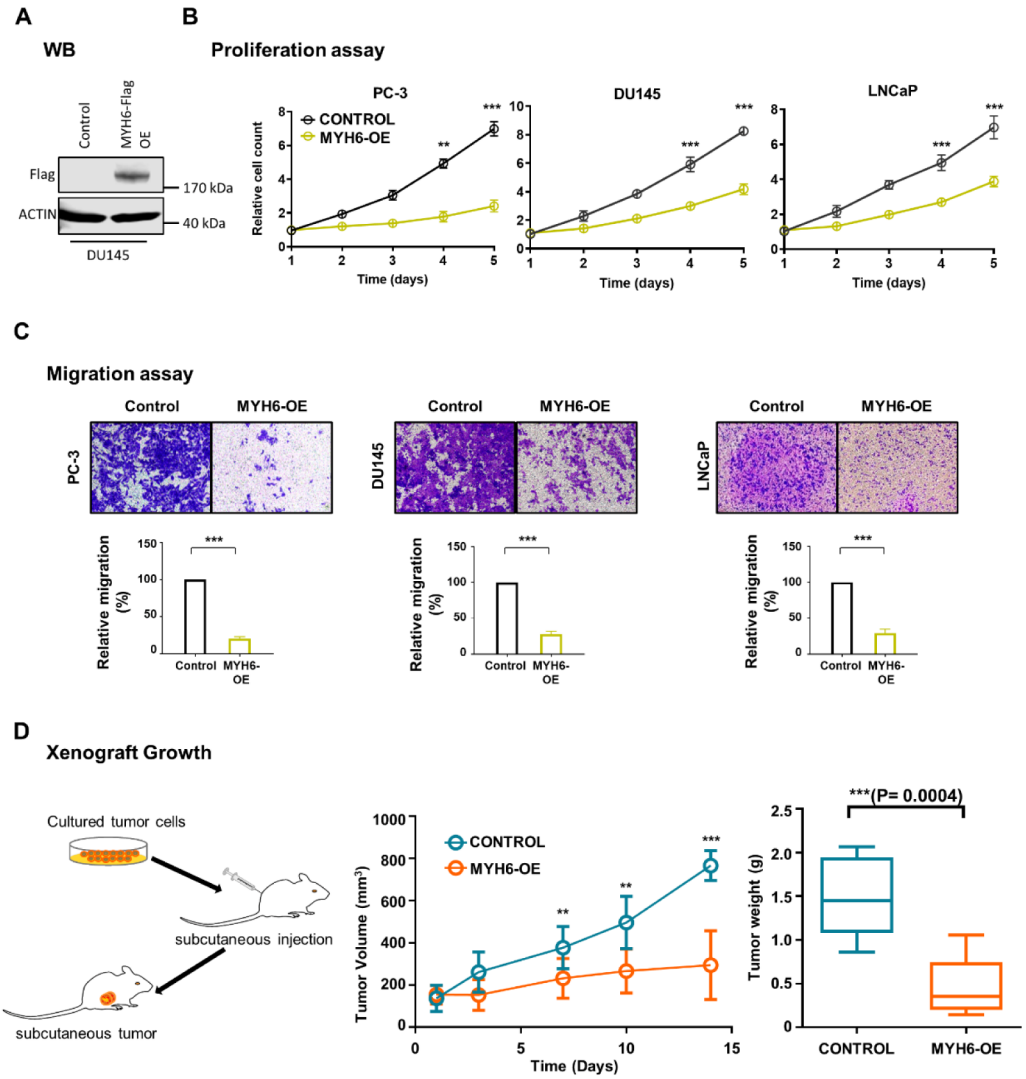

Fig. 3. MYH6 suppresses prostate cancer cell proliferation and migration. (**A**) Western blotting showed the protein levels in the indicated cell lines with MYH6 overexpression. (**B**) Cell proliferation was measured at the indicated time points in LNCaP, PC-3 and DU145 cells (**P < 0.01, ***P < 0.001, N = 3). (**C**) Transwell assay analyses of the indicated cell lines (N = 3). (**D**) Xenograft analyses of DU145-derived tumors with control vector or MYH6 overexpression (**P < 0.01, ***P < 0.001).

MYH6 suppresses cell proliferation and migration via downregulation of KIT expression in prostate cancer

Through the study above, we validated that MYH6 could suppress prostate cancer development. In the next step, we tried to determine the underlying mechanisms. DU145 and PC-3 cells are androgen-independent prostate cancer cells. DU145 is considered the most malignant among common the prostate cancer cell lines, and is primarily used to study the progression of advanced hormone-independent prostate cancer. In our previous study, we found that MYH6 expression is lower in more malignant prostate cancers, suggesting that further suppression of MYH6 function is needed to promote tumor progression. Therefore, we chose to study the most malignant DU145 cell lines for subsequent mechanistic studies. To elucidate the downstream genes regulated by MYH6 in prostate cancer, we conducted RNA-seq analysis on both control and MYH6-overexpressing DU145 cell lines. A total of 747 genes displaying significant differential expression were identified across the experimental groups (Fig. 4A). In total, 305 DEGs were upregulated in the MYH6-overexpressing group, whereas 442 genes were downregulated (Supplementary Table S1). To delve deeper into the functional roles of these DEGs, we conducted gene functional enrichment analysis using the online tool DAVID. We uploaded all the DEGs and performed Gene Ontology (GO) and KEGG analyses. The results showed that the DEGs were enriched in the regulation of ion transmembrane transport, negative regulation of neuron apoptotic process, muscle organ development, potassium ion transmembrane transport, forebrain neuron differentiation, neuron development, response to ischemia, regulation of vasoconstriction, cell adhesion, cardiac muscle contraction, branching involved in ureteric bud

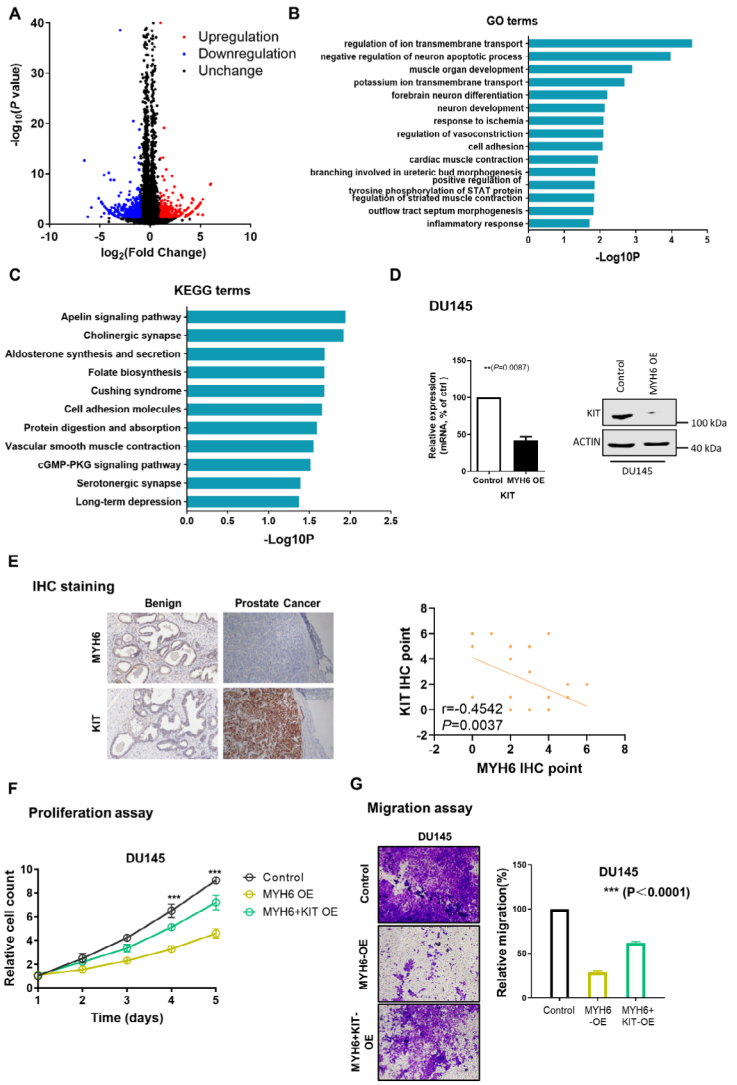

Fig. 4. MYH6 suppresses prostate cancer cell proliferation and migration by repressing KIT expression. (**A**) Volcano plot for DEGs in MYH6-overexpressing DU145 RNA-seq. (**B**) The GO enrichment terms of DEGs. (**C**) KEGG pathway analysis of DEGs. (**D**) RT-qPCR analyses of the mRNA levels and western blotting analysis of protein levels of the KIT gene in prostate cancer cells with a control vector or MYH6 overexpression. (**E**) Representative immunohistochemistry of MYH6 and KIT on benign prostate and prostate cancer tissues. (**F**) KIT overexpression rescued the MYH6-mediated decrease in cell proliferation in DU145 cells. One-way ANOVA was used. (**G**) KIT overexpression rescued MYH6-mediated defects in cell migration (**P < 0.01, ***P < 0.001).

morphogenesis, positive regulation of tyrosine phosphorylation of STAT protein, regulation of striated muscle contraction, outflow tract septum morphogenesis, and inflammatory response (Fig. 4B). In the pathway analysis, we found that the DEGs were enriched mainly in the apelin signaling pathway, cholinergic synapse, aldosterone synthesis and secretion, folate biosynthesis, Cushing syndrome, cell adhesion molecules, protein digestion and absorption, vascular smooth muscle contraction, cGMP-PKG signaling pathway, serotonergic synapse, long-term depression, calcium signaling pathway, oxytocin signaling pathway, cortisol synthesis and secretion, and neutrophil extracellular trap formation (Fig. 4C).

Among all the DEGs, we focused on KIT, which is a critical oncogene that contributes to tumor progression in pathological conditions[24]. Previous studies showed that KIT-positive prostate cancer samples exhibited a trend toward a higher risk of relapse[25]. KIT is associated with the downregulation of BRCA2 and promotes bone metastasis in prostate cancer[26]. Additionally, KIT is regulated by FOXA2 and is involved in neuroendocrine prostate cancer (NEPC)[27]. In this study, we found that KIT expression was significantly downregulated upon MYH6 overexpression, which was also confirmed by qPCR and western blotting assays (Fig. 4D). Furthermore, analysis of IHC using our own tissues also revealed a negative correlation between MYH6 and TGFA expression (Fig. 4E). We then tried to validate whether downregulation of KIT could mediate the tumor suppressor role of MYH6 in prostate cancer. We then overexpressed KIT in DU145 cells. Overexpression of KIT partially

rescued the decrease in cell proliferation caused by MYH6 upregulation in DU145 cells (Fig. 4F). Moreover, KIT overexpression also resulted in the recovery of migration ability in MYH6-upregulated DU145 cells (Fig. 4G). These findings collectively suggest that MYH6 inhibits the proliferation and migration of prostate cancer cells by reducing the expression of KIT.

Discussion

Prostate cancer is the leading malignant tumor in males worldwide, especially in Western countries[28]. In this study, we illustrate that MYH6 expression is reduced in prostate cancer through bioinformatic analyses and immunohistochemical assessment, highlighting the potential involvement of MYH6 in prostate cancer.

The identification of MYH6 relied on our previous results and the gene expression data from authoritative prostate cancer databases. Bioinformatic analysis is currently a very important tool, as evidenced by many similar studies. Through comprehensive single-cell sequencing analysis, a previous study identified type I collagen-secreting tumor-associated fibroblasts and found that they are key mediators in metastatic brain tumors, uncovering tumor receptors potentially associated with patient survival[29]. Another study identified two distinct subsets within the inflammatory Th17 cell compartment and discovered their respective regulatory mechanisms[30]. In these studies, bioinformatics approaches can help discover potential important pathogenic genes and mechanisms, guiding the research direction. Similarly, our research identified the potential important function of MYH6 in prostate cancer through bioinformatics analysis. Subsequent analysis revealed the tumor suppressor function of MYH6 in prostate cancer, a finding corroborated by both in vitro, in vivo assays, and IHC in tumor tissues. We found that MYH6 could inhibit the proliferation and migration of prostate cancer cells and is closely related to disease staging and prognosis. This suggests the potential importance of MYH6 in the clinical diagnosis and prognosis assessment of prostate cancer. In the future, doctors could determine the expression level and ratio of MYH6 in tissue samples obtained through surgery or biopsy, which could help determine the stage of prostate cancer and assist in the preliminary prognosis assessment. Additionally, with continuous innovations in diagnostic techniques, such as genetic testing for diseases and the development of potential targeted drugs for MYH6, we could select more personalized and precise treatment methods based on the patient's MYH6 expression levels and mutation status. Additionally, the results of the prognostic analysis indicated that patients with lower MYH6 expression may benefit from early intervention because of the poorer prognosis. As research progresses, the clinical application of MYH6 in prostate cancer will become more extensive.

We also identified the downstream genes of MYH6 in disease progression. We focused on the KIT gene, which encodes a receptor tyrosine kinase[24]. KIT was first recognized as a counterpart to the feline sarcoma viral oncogene V-KIT and is commonly denoted as proto-oncogene C-KIT[24]. Prior studies have shown that KIT is pivotal in regulating the proliferation, differentiation, migration, and apoptosis across various cell types, thereby exerting a significant influence on processes such as hematopoiesis, stem cell maintenance, gametogenesis, melanogenesis, as well as mast cell development, migration, and function[24,31–34]. Here, we found that KIT expression was much lower when MYH6 was overexpressed in prostate cancer cells. Due to the important roles of KIT in tumor progression, we suggest that KIT might mediate the critical tumor suppressor role of MYH6 in this progression. Some previous results indicated the potential role of MYH6 in multiple cancer types, but no concrete mechanisms were discovered. Previous cancer research has found that MYH6 is significantly downregulated in head and neck squamous cell carcinoma[5]. In small cell lung cancer (SCLC), MYH6 frequently mutates in chemotherapy-treated residual tumors, which might contribute to chemoresistance and influence the prognosis of patients[6]. However, the specific mechanisms have not been explored, and no clear downstream pathways have been identified. In our study, we clearly demonstrated the tumor-suppressive role of MYH6 in the progression of prostate cancer and explored downstream pathways and related mechanisms through RNA-seq and other methods. Our results indicate that the KIT pathway is a potential downstream gene and pathway in prostate cancer, although the direct regulatory pattern has still not been clearly described. In future research, we will continue to explore the mechanisms by which MYH6 regulates KIT and other genes and determine the noncardiac role of MYH6 in disease status.

Our study contained several limitations. Many of our findings are preliminary, including the mechanisms underlying MYH6 downregulation in prostate cancer. In forthcoming studies, we intend to employ molecular biological experiments to corroborate our results.

Conclusions

In conclusion, our findings indicate a significant downregulation of MYH6 expression in prostate cancer tissue, which correlates with poorer clinical outcomes. Overexpression of MYH6 significantly influences the proliferation and migration of prostate cancer cells. Moreover, we found that KIT is the downstream gene of MYH6 during disease progression. Collectively, our findings provide the initial evidence of the tumor suppressor role of MYH6 in prostate cancer. This implies that MYH6 holds significant promise as a therapeutic target in prostate cancer treatment.

Data availability

All data generated or analyzed during this study are included in this published article and its supplementary information files.

Received: 22 May 2024; Accepted: 20 August 2024
Published online: 24 August 2024

References

1. Siegel, R. L., Miller, K. D. & Jemal, A. Cancer statistics, 2016. *CA. Cancer J. Clin.* **66**, 7–30. https://doi.org/10.3322/caac.21332 (2016).
2. Weiss, A., Schiaffino, S. & Leinwand, L. A. Comparative sequence analysis of the complete human sarcomeric myosin heavy chain family: Implications for functional diversity. *J. Mol. Biol.* **290**, 61–75 (1999).
3. Chen, J.-H. *et al.* Identification of MYH6 as the potential gene for human ischaemic cardiomyopathy. *J. Cell. Mol. Med.* **25**, 10736–10746. https://doi.org/10.1111/jcmm.17015 (2021).
4. Zhou, L., Liu, Y., Lu, L., Lu, X. & Dixon, R. A. Cardiac gene activation analysis in mammalian non-myoblasic cells by Nkx2-5, Tbx5, Gata4 and Myocd. *PLoS One* **7**, e48028 (2012).
5. Li, C. *et al.* Analysis of myosin genes in HNSCC and identify MYL1 as a specific poor prognostic biomarker, promotes tumor metastasis and correlates with tumor immune infiltration in HNSCC. *BMC Cancer* **23**, 840. https://doi.org/10.1186/s12885-023-11349-5 (2023).
6. Yu, J. *et al.* Whole exome analysis reveals the genomic profiling related to chemo-resistance in Chinese population with limited-disease small cell lung cancer. *Cancer Med.* **12**, 1035–1050. https://doi.org/10.1002/cam4.4950 (2023).
7. Sun, J., Li, S., Wang, F., Fan, C. & Wang, J. Identification of key pathways and genes in PTEN mutation prostate cancer by bioinformatics analysis. *BMC Med. Genet.* **20**, 1–9 (2019).
8. Sun, J. *et al.* Identification of critical pathways and hub genes in TP53 mutation prostate cancer by bioinformatics analysis. *Biomark. Med.* **13**, 831–840 (2019).
9. Robinson, M. D., McCarthy, D. J. & Smyth, G. K. edgeR: A Bioconductor package for differential expression analysis of digital gene expression data. *Bioinformatics* **26**, 139–140. https://doi.org/10.1093/bioinformatics/btp616 (2010).
10. McCarthy, D. J., Chen, Y. & Smyth, G. K. Differential expression analysis of multifactor RNA-Seq experiments with respect to biological variation. *Nucleic Acids Res.* **40**, 4288–4297. https://doi.org/10.1093/nar/gks042 (2012).
11. Ke, A. W. *et al.* CD151 amplifies signaling by integrin α6β1 to PI3K and induces the epithelial–mesenchymal transition in HCC cells. *Gastroenterology* **140**, 1629-1641.e1615 (2011).
12. Huang, X. Y. *et al.* alphaB-crystallin complexes with 14–3-3zeta to induce epithelial-mesenchymal transition and resistance to sorafenib in hepatocellular carcinoma. *Hepatology* **57**, 2235–2247. https://doi.org/10.1002/hep.26255 (2013).
13. Wang, J. *et al.* LanCL1 protects prostate cancer cells from oxidative stress via suppression of JNK pathway. *Cell Death Dis.* **9**, 197. https://doi.org/10.1038/s41419-017-0207-0 (2018).
14. Dai, D. L., Martinka, M. & Li, G. Prognostic significance of activated Akt expression in melanoma: A clinicopathologic study of 292 cases. *J. Clin. Oncol.* **23**, 1473–1482. https://doi.org/10.1200/JCO.2005.07.168 (2005).
15. Wang, J. *et al.* HNF1B-mediated repression of SLUG is suppressed by EZH2 in aggressive prostate cancer. *Oncogene* **39**, 1335–1346. https://doi.org/10.1038/s41388-019-1065-2 (2020).
16. Kong, L. *et al.* A primary role of TET proteins in establishment and maintenance of De Novo bivalency at CpG islands. *Nucleic Acids Res.* **44**, 8682–8692. https://doi.org/10.1093/nar/gkw529 (2016).
17. Wang, J. *et al.* Overexpression of WDFY2 inhibits prostate cancer cell growth and migration via inactivation of Akt pathway. *Tumour Biol.* **39**, 1010428317704821. https://doi.org/10.1177/1010428317704821 (2017).
18. Dennis, G. Jr. *et al.* DAVID: Database for annotation, visualization, and integrated discovery. *Genome Biol.* **4**, P3 (2003).
19. Kanehisa, M. & Goto, S. KEGG: Kyoto encyclopedia of genes and genomes. *Nucleic Acids Res.* **28**, 27–30. https://doi.org/10.1093/nar/28.1.27 (2000).
20. Kanehisa, M. Toward understanding the origin and evolution of cellular organisms. *Protein Sci.* **28**, 1947–1951. https://doi.org/10.1002/pro.3715 (2019).
21. Kanehisa, M., Furumichi, M., Sato, Y., Kawashima, M. & Ishiguro-Watanabe, M. KEGG for taxonomy-based analysis of pathways and genomes. *Nucleic Acids Res.* **51**, D587–D592. https://doi.org/10.1093/nar/gkac963 (2023).
22. Reiner, A., Yekutieli, D. & Benjamini, Y. Identifying differentially expressed genes using false discovery rate controlling procedures. *Bioinformatics* **19**, 368–375 (2003).
23. Benjamini, Y., Drai, D., Elmer, G., Kafkafi, N. & Golani, I. Controlling the false discovery rate in behavior genetics research. *Behav. Brain Res.* **125**, 279–284 (2001).
24. Lennartsson, J., Jelacic, T., Linnekin, D. & Shivakrupa, R. Normal and oncogenic forms of the receptor tyrosine kinase kit. *Stem Cells* **23**, 16–43 (2005).
25. Di Lorenzo, G. *et al.* Expression of proto-oncogene c-kit in high risk prostate cancer. *Eur. J. Surg. Oncol. (EJSO)* **30**, 987–992. https://doi.org/10.1016/j.ejso.2004.07.017 (2004).
26. Mainetti, L. E. *et al.* Bone-induced c-kit expression in prostate cancer: A driver of intraosseous tumor growth. *Int. J. Cancer* **136**, 11–20. https://doi.org/10.1002/ijc.28948 (2015).
27. Han, M. *et al.* FOXA2 drives lineage plasticity and KIT pathway activation in neuroendocrine prostate cancer. *Cancer Cell* **40**, 1306-1323.e1308. https://doi.org/10.1016/j.ccell.2022.10.011 (2022).
28. Bray, F. *et al.* Global cancer statistics 2018: GLOBOCAN estimates of incidence and mortality worldwide for 36 cancers in 185 countries. *CA. Cancer J. Clin.* **68**, 394–424. https://doi.org/10.3322/caac.21492 (2018).
29. Song, Q. *et al.* Single-cell sequencing reveals the landscape of the human brain metastatic microenvironment. *Commun. Biol.* **6**, 760. https://doi.org/10.1038/s42003-023-05124-2 (2023).
30. Bouch, R. J. *et al.* Distinct inflammatory Th17 subsets emerge in autoimmunity and infection. *J. Exp. Med.* https://doi.org/10.1084/jem.20221911 (2023).
31. Yasuda, A. *et al.* The stem cell factor/c-kit receptor pathway enhances proliferation and invasion of pancreatic cancer cells. *Mol. Cancer* **5**, 1–10 (2006).
32. Mauduit, C., Hamamah, S. & Benahmed, M. Stem cell factor/c-kit system in spermatogenesis. *Hum. Reprod. Update* **5**, 535–545 (1999).
33. Deshpande, S. *et al.* Kit ligand cytoplasmic domain is essential for basolateral sorting in vivo and has roles in spermatogenesis and hematopoiesis. *Dev. Biol.* **337**, 199–210 (2010).
34. Lim, K.-H., Pardanani, A. & Tefferi, A. KIT and mastocytosis. *Acta Haematol.* **119**, 194–198 (2008).

Acknowledgements

KEGG pathway database is copyrighted by Kanehisa laboratories and we have formal permission from them to publish this material commercially under an Open Access license.

Author contributions

JQW, FW and JS: conception and design and drafting the manuscript; JS: obtaining funding; JQW, FW and KL: acquisition of the data and drafting the manuscript; JQW and FW: in vitro and in vivo assays; JS, HS and YHD: critical revision of the manuscript; HS, YHD and JQW: statistical analysis and technical support.

Funding
The authors acknowledged receiving financial assistance for conducting, writing, and/or publishing this article as follows: This research received funding from the Suzhou Youth Project of Science and Education for Medicine (grant no. SKJY2021127) and the Suzhou Urological Disease Clinical Medical Center (grant no. Szlcyxzx202106).

Competing interests
The authors declare no competing interests.

Additional information
Supplementary Information The online version contains supplementary material available at https://doi.org/10.1038/s41598-024-70665-3.

Correspondence and requests for materials should be addressed to J.W. or J.S.